AJNR Am J Neuroradiol 20:501–507, March 1999

Characterization of Differences between Multiple Sclerosis and Normal Brain: A Global Magnetization Transfer Application

John L. Ostuni, Nancy D. Richert, Bobbi K. Lewis, and Joseph A. Frank

BACKGROUND AND PURPOSE: **Although the exact nature of the physiological differences between normal and multiple sclerosis (MS) brains are unknown, it has been shown that their global magnetization transfer ratio (MTR) values are significantly different. To more fully understand these differences, we examined MTR values by using 30 distinct measures. We provide a unique illustration of these differences through a derived normal-to-MS transform.**

METHODS: **Global MTR values for the group of normal subjects and for the group of MS subjects were characterized by 30 different measures involving simple statistics, histographic characteristics, MTR order information, and MTR range information. The measures that were significantly different with respect to these two groups were discovered. From the mean MTR histogram of the two groups, a transform was created to describe a conversion between the two brain states. Normal data were passed through this transform, creating a set of pseudo-MS data. The measures that were significantly different from the normal and pseudo-MS data were also obtained in order to verify the accuracy of the transform.**

RESULTS: **Seventeen of the 30 measures were determined to be significantly different when comparing the sets of normal and MS data. The same set of 17 measures were found to be significantly different when comparing the normal and pseudo-MS data.**

CONCLUSION: **The differences in the global MTR values of normal and MS subjects are statistically significant compared with a large number of measures ($\alpha = 0.05$). A normal-to-MS transform is a novel method for illustrating these differences.**

Magnetization transfer is a technique that may be useful in characterizing the pathophysiological changes involved with multiple sclerosis (MS). Typically, mean magnetization transfer ratio (MTR) values are collected from white matter hyperintensities and normal-appearing white matter by using small regions of interest (1–12). A global approach based on histograms has been used to more accurately represent occult disease in normal-appearing white matter (13, 14). Characteristics of these histograms have been correlated with cognitive and neuropsychological test results (15) and have been used to evaluate changes in response to treatment (16).

Received May 14, 1998; accepted after revision November 10.

Presented in part as a poster at the annual meeting of the International Society for Magnetic Resonance, Vancouver, April 1997.

From the Laboratory of Diagnostic Radiology Research, National Institutes of Health, Bethesda, MD.

Address reprint requests to John Ostuni, PhD, National Institutes of Health, Building 10, Room B1N256, 10 Center Dr, MSC 1074, Bethesda, MD 20892.

In this report, the difference between MS and normal subject groups with respect to these global MTR values was explored through the use of 30 different measures. These measures included the following: 1) simple statistics, such as MTR mean and standard deviation (SD); 2) range measures that were associated with properties of the set of MTR values within a specific range, such as the number of voxels with an MTR value between 0.45 and 0.60; 3) order measures that were associated with properties of MTR values after they were ordered in terms of their magnitude, such as the mean MTR in the quarter of the data containing the smallest MTR values; and 4) histographic measures that were associated with properties of the MTR histogram, such as mode and peak height. The mean value of each of these 30 measures was determined for each normal and MS subject. Statistical testing of these mean values was then performed to find which measures were significantly different between the two groups.

Finally, to provide a single illustrative technique for describing the differences between these two groups, a transform relating the set of normal subjects to the set of MS subjects was created through

the matching of each group's mean MTR histogram. This normal-to-MS transform converts the set of normal MTR values into a set of MTR values typical of the MS data set. By putting each normal MTR volume through this transform, all normal data were converted into pseudo-MS data. The descriptive ability of this transform was examined by performing the same analysis on the normal and pseudo-MS groups as was performed on the normal and MS groups.

Methods

Studies were performed on a 1.5-T MR unit and consisted of axial oblique 3-mm interleaved sections (n = 42), with a field of view of 24 cm and a matrix of 256 × 192. For magnetization transfer studies, spin-echo images were obtained with imaging parameters of 600/16/2 (TR/TE/excitations), with (Ms) and without (Mo) a saturation pulse (600 MHz below water frequency B_1). All other parameters were set according to manufacturer's specifications. The MTR was computed on a voxel-by-voxel basis using the standard equation: 1 − (Ms/Mo) (1). Thirteen subjects (five normal volunteers, eight MS patients) were analyzed. The normal subjects (three men, two women; mean age, 37 years; range, 23–44 years) had an average of 4.2 studies per subject. The MS subjects (two men, seven women; mean age, 37 years; range, 24–44 years; Kurtze Expanded Disability Status Scale: range, 1–8; disease duration: range, 1–9 years; and minimum contrast-enhancing lesion frequency, 0.5/month) had an average of 9.4 studies per subject. The MS patients were part of a longitudinal MR imaging study of relapsing-remitting MS (17). This study was reviewed and approved by the institutional review board at the National Institutes of Health. Informed consent was obtained for each normal volunteer and MS patient.

Initially, a mapfile was created for each subject by removing the skull and extradural tissues in the Mo volume from their first examination. A mapfile or image mask is simply a set of images that describe which voxel locations need to be analyzed and which voxel locations should be ignored in the analysis of a subject's brain. This task was performed by an experienced radiologist through the use of hand-drawn outlines. All subsequent intrasubject Mo and Ms volumes were registered (18) to this first Mo volume, so that a single mapfile could be used for all intrasubject MR data. After registration, each Mo-Ms pair was used to create a new volume whose voxel values were equal to their MTR at that location. This volume was then masked with the created mapfile to form an MTR volume.

For each subject in both groups, the mean of each of the 30 investigated measures was calculated. Thus, this report does not examine the monthly fluctuations in MS and normal brains, but instead compares the average individual brain state of each subject in the two groups. These mean values for the normal control subjects and MS subjects were compared by the Wilcoxon rank sum test (19) to determine which measures were significantly different ($\alpha = 0.05$).

Notation

Let mapfile_j, Mo_j, and Ms_j represent the value of the mapfile, the Mo volume, and the Ms volume at voxel position j, where j goes from 1 to the total number of voxels in a volume. For all voxels in an Ms volume, if at a particular voxel, j, the following conditions are true, ie,

$$\text{mapfile}_j = 1$$

$$\text{Mo}_j \neq 0$$

$$(1 - \text{Ms}_j/\text{Mo}_j) \geq 0.0 \text{ and } (1 - \text{Ms}_j/\text{Mo}_j) < 0.6,$$

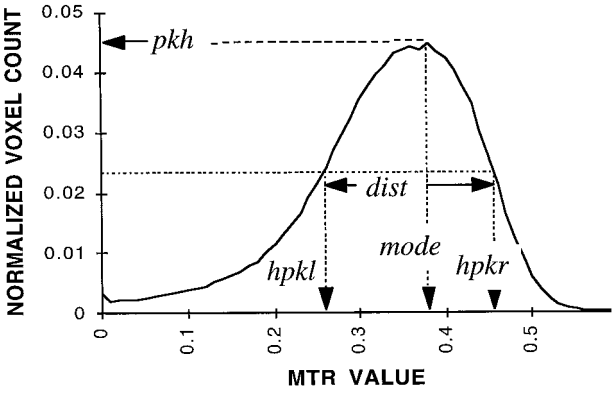

FIG 1. Typical "normal" MTR histogram shows the parameters H1 through H5.

then that MTR value is added to the set of MTR values to be analyzed. We will refer to this set of values from a single Mo-Ms pair as S and the total number of MTR values composing this set as N. Also, each individual element in S will be referred to as s_j where j goes from 1 to N. The choice of 0.6 as a cutoff was determined empirically from the observation that almost no voxels contain an MTR value greater than this value.

MTR Measures I (Histographic Parameters)

To globally characterize MTR values, it is useful to store them in a histogram (20) (Fig 1). For this analysis, a histogram, referred to as *histo*[ ], contained 100 bins, with each bin representing an MTR range of .006 (0.6/100). Initially, all elements were set to 0. For each MTR value in the set S, the following quantity was incremented:

$$histo\left[int\left(\frac{100}{0.6}S_j\right)\right],$$

where S_j refers to the individual MTR values and the function *int*( ) converts a noninteger number to an integer through truncation. Once the histogram was created, the following measures were calculated:

H1. mode: the parameter mode characterizes the bin number at the maximum height of the histogram; that is, the histogram bin containing the most MTR values;

H2. pkh: the peak height (pkh) is estimated as the number of MTR values contained in the histogram bin representing the mode;

H3, H4. hpkl, hpkr: these two parameters represent the bin numbers of the two locations where the histogram makes the transition from a height of greater than pkh/2 to a height less than or equal to pkh/2; hpkl represents the location to the left of the mode and hpkr represents the location to the right of the mode;

H5. dist: this parameter represents the number of bins between hpkl and hpkr;

H6. modep: this parameter represents the percentage of the total number of MTR values in the bin range of 0 to mode;

H7. pkhn: this parameter represents the normalized peak height = pkh/N;

H8, H9. hpklp, hpkrp: these two parameters represent the percentage of the total number of MTR values in the bin ranges 0 to hpkl and 0 to hpkr, respectively;

H10. distp: this parameter represents the percentage of the total number of MTR values in the bin range of hpkl to hpkr.

MTR Measures II (Simple Statistical Parameters)

Initially, simple group statistics were applied to the collection of MTR values. Using the *N* members of each set, S, the measures S1 to S4 were found. These measures were all common measures, such as the mean, which measures the average value of the set of MTR values, and the SD, which characterizes the variability of the MTR values around the mean. Also calculated were the skew, which measures the degree of asymmetry around the mean, and the kurtosis, which measures the relative flatness of the MTR collective compared with a normal distribution centered around the mean:

S1. $$\text{mean} = \frac{1}{N}\sum_{j=1}^{N} S_j$$

S2. $$\text{sd} = \left(\frac{1}{N-1}\sum_{j=1}^{N} (S_j - \text{mean})^2\right)^{1/2}$$

S3. $$\text{skew} = \frac{1}{N(\text{sd})^3}\sum_{j=1}^{N} (S_j - \text{mean})^3$$

S4. $$\text{kurtosis} = \frac{1}{N(\text{sd})^4}\sum_{j=1}^{N} (S_j - \text{mean})^4$$

MTR Measures III (Range Parameters)

The next eight parameters (R1–R8) were based on MTR-range quartiles that were formed by dividing the MTR range (0.0–0.60) into four equal parts. The normalized parameters R5 to R8 were normalized by *N*, the number of brain voxels having an MTR value between 0.0 and 0.6. In general, non-normalized parameters provide information on the absolute quantities of MTR values, while normalized parameters provide information on the relative quantities of MTR values:

R1. c1: number of voxels with an MTR value in the range (0.00–0.15);

R2. c2: number of voxels with an MTR value in the range (0.15–0.30);

R3. c3: number of voxels with an MTR value in the range (0.30–0.45);

R4. c4: number of voxels with an MTR value in the range (0.45–0.60);

R5. c1n: normalized number of voxels with an MTR value in the range (0.00–0.15) = c1/*N*;

R6. c2n: normalized number of voxels with an MTR value in the range (0.15–0.30) = c2/*N*;

R7. c3n: normalized number of voxels with an MTR value in the range (0.30–0.45) = c3/*N*;

R8. c4n: normalized number of voxels with an MTR value in the range (0.45–0.60) = c4/*N*.

MTR Measures IV (Order Parameters)

One common data structure, which has not previously been used for examining sets of MTR values, is the sorted data array. The matrix sortarr[ ] contains *N* elements representing the ordered MTR values from the set *S*. This array was divided into four equal parts to form MTR-count quartiles, in comparison with the previous discussion involving MTR-range quartiles. The following parameters, O1 to O8, were estimated through the use of these MTR-count quartiles (Fig 2) and are concerned with the mean and the range of each of these four quartiles:

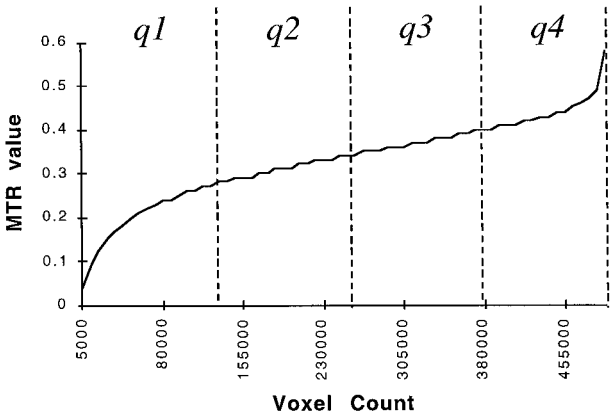

FIG 2. Typical "normal" array of ordered MTR values, with *dotted lines* showing the four evenly spaced quadrants used to derive parameters O1 through O8. These parameters simply find the mean and the range of each of the four count-based quadrants.

O1. mn1: mean of the first *N*/4 data points;

O2. mn2: mean of the second *N*/4 data points;

O3. mn3: mean of the third *N*/4 data points;

O4. mn4: mean of the fourth *N*/4 data points;

O5. rg1: (highest MTR value − lowest MTR value) in first *N*/4 data points;

O6. rg2: (highest MTR value − lowest MTR value) in second *N*/4 data points;

O7. rg3: (highest MTR value − lowest MTR value) in third *N*/4 data points;

O8. rg4: (highest MTR value − lowest MTR value) in fourth *N*/4 data points.

Normal to MS Transform

The MTR histogram is a data structure that allows for the examination of the number of MTR values falling within specific ranges. This data structure is basically a one-dimensional array in which each array element represents a specific MTR range. In the context of a histogram, these array elements are called bins. For every MTR value examined, the bin representing that value is incremented by 1.

A group's mean histogram is a histogram created using all of that group's MTR data. Thus, it allows one to examine the number of MTR values falling within specific ranges for all of that group's data. In this report, the mean MTR histogram of the normal subject group was compared with the mean MTR histogram of the MS patient group (Fig 3) to derive a transform (Fig 4) representing the differences between the two groups. This transform will be referred to as a normal-to-MS transform.

All MTR volumes from the normal subject group (average, 4.2 MTR volumes/normal subject) were put through this normal-to-MS transform to arrive at the group of pseudo-MS data

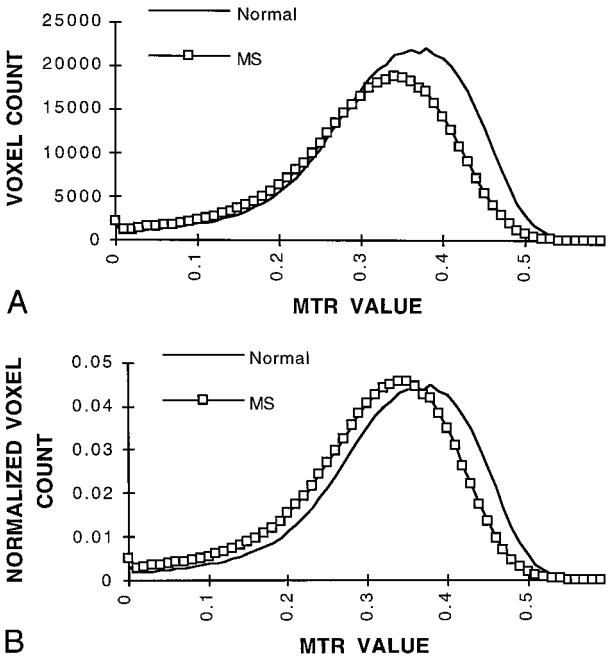

FIG 3. Mean MTR histograms for the normal volunteer group and the MS subject group.

A and *B*, Nonnormalized MTR histograms (*A*) and normalized MTR histograms (*B*).

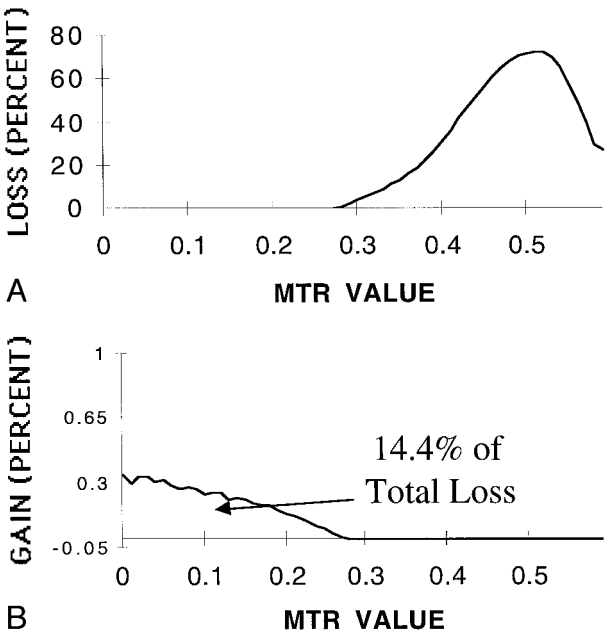

FIG 4. *A* and *B*, Normal-to-MS transform. Loss described by the normal-to-MS transform (*A*) and gain described by the normal-to-MS transform (*B*). For example, in transforming a normal brain to one representative of the MS data set, approximately 75% of all voxels with an MTR value of 0.5 are removed; 14.4% of them are relocated to lower MTR values in a distribution shown in *B*, while 85.6% of them are lost. A similar action is performed for voxels with MTR values at other values, although the percentage of loss differs, as shown in *A*.

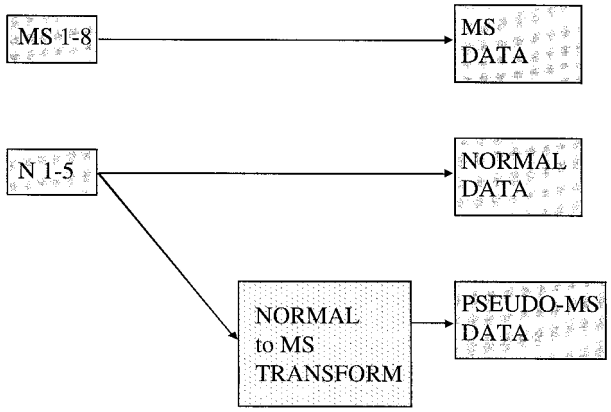

FIG 5. Illustration of the three data sets that were used in this study. The last data set (pseudo-MS) was created by putting each of the normal subjects' MTR data through a derived normal-to-MS transform. Since five normal subjects had an average of 4.2 studies each, 21 MTR volumes were transformed in the creation of the five pseudo-MS subjects. The normal-to-MS transform was created through the matching of the mean MTR histograms of the normal data (labeled N *1–5*) and the MS data (labeled *MS 1–8*).

(Fig 5). Thus, the five normal subjects were converted into five pseudo-MS subjects. The mean value of each of the examined 30 measures was found for each subject in this new pseudo-MS group just as they were for the normal and MS groups. Using the Wilcoxon rank sum test, these measures were compared with those of the normal group to discover which of the measures were significantly different ($\alpha = 0.05$). In summary, the analysis between the normal and pseudo-MS groups was identical to that of the normal and MS groups.

Results

With regard to the comparison of normal and MS subjects, 17 of 30 measures were statistically significant using an α value of 0.05 (Fig 6). Of these 17 measures, nine were found that could be used to state differences between the normal subject group and the MS patient groups using an α value of 0.001. A complete list of these *P* values along with their direction of change is presented in the Table.

In considering the groups of MS and normal subjects from the four simple statistical parameters (S1–S4), only the mean that describes the average MTR value has significantly decreased. The other three parameters (ie, SD, skew, and kurtosis) were not changed significantly.

The range parameters c3 and c4 describe a decrease in the total number of voxels with MTR values in the range (0.30–0.60). To further understand this reduction, it is informative to examine the normalized quadrant counts, c1n, c2n, c3n, and c4n. These normalized parameters suggest a relative loss of voxels with high MTR values (0.30–0.60) and a relative gain of voxels with lower values (0.00–0.30). Thus, while no significant increase is found in the number of voxels representing lower MTR values, a significant increase is found in the percentage of the brain made up of these voxels. This finding is in contrast to the higher MTR values, in

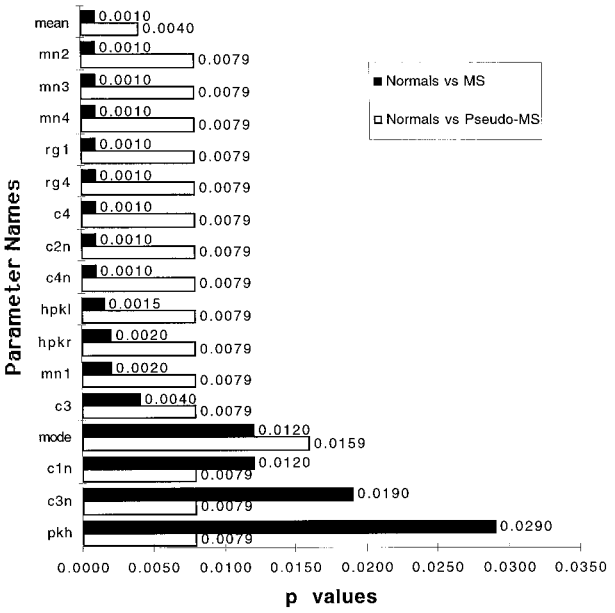

FIG 6. *P* values associated with the comparison of the measures shown with respect to normal and MS subjects (*filled bars*) and with respect to normal subjects and pseudo-MS subjects (*open bars*). All unlisted measures had *P* values greater than .05.

which a significant loss is found in both the number of voxels representing these values and the percentage of the brain made up of these voxels, and is consistent with the brain atrophy that has been observed in MS patients (21).

To obtain more information on these changes, the parameters resulting from the ordered MTR values (O1–O8) can be examined. The mean values for all four quarters of the data (mn1, mn2, mn3, and mn4) illustrate that, in MS subjects, each of these means is significantly lower than which occurs in normal subjects. This difference suggests a relative increase in the number of voxels represented by low MTR values. The increase in parameter rg1 verifies that the majority of this increase must be in the first *N*/4-ordered MTR values (typically from 0.0 to approximately 0.20). The parameter rg4 further shows that the maximum MTR value in MS subjects appears to decrease at a slower rate than the average MTR value in the fourth *N*/4-ordered MTR values, implying that not all voxels with a high MTR value are affected equally.

The histogram parameters (mode, pkh, hpkl, and hpkr) all significantly decrease in the MS group compared with the normal group. Interestingly, the change in all four of these parameters can be explained by the loss of voxels with MTR values in the range (0.30–0.60) without regard for the gain of voxels with lower MTR values.

With regard to the comparison of normal and pseudo-MS subjects, the exact same measures were found to have significantly changed as were found in the comparison of the normal and MS data sets. In addition, all 17 of these measures changed in the same direction. Thus, the differences depicted by the normal MTR data and the transformed normal

***P* values and their direction of change**

Parameter Name	Normal vs MS Subjects	Normal vs Pseudo-MS Subjects	Change
H1: mode	.0120	.0159	Decrease
H2: pkh	.0290	.0079	Decrease
H3: hpk1	.0015	.0079	Decrease
H4: hpkr	.0020	.0079	Decrease
H5: dist	.2373	.1667	…
H6: modep	.4376	1.0000	…
H7: pkhn	.7972	.2222	…
H8: hpklp	.1898	.0952	…
H9: hpkrp	.1469	.4206	…
H10: distp	.1119	.0952	…
S1: mean	.0010	.0040	Decrease
S2: sd	.6993	.4206	…
S3: skew	.3636	.6905	…
S4: kurt	.4101	.7302	…
R1: c1	.4376	.0952	…
R2: c2	.3636	.4206	…
R3: c3	.0040	.0079	Decrease
R4: c4	.0010	.0079	Decrease
R5: c1n	.0120	.0079	Increase
R6: c2n	.0010	.0079	Increase
R7: c3n	.0190	.0079	Decrease
R8: c4n	.0010	.0079	Decrease
O1: mn1	.0020	.0079	Decrease
O2: mn2	.0010	.0079	Decrease
O3: mn3	.0010	.0079	Decrease
O4: mn4	.0010	.0079	Decrease
O5: rg1	.0010	.0079	Increase
O6: rg2	.8981	.1508	…
O7: rg3	.3636	.3095	…
O8: rg4	.0010	.0079	Decrease

Note.—*P* values associated with the comparison of the measures shown with respect to normal subjects and MS subjects (second column) and with respect to normal subjects and pseudo-MS subjects (third column). The direction of change for the significantly different measures ($P < .05$) is shown in column 4 (see Methods for a discussion of each parameter). The direction of change for all significantly different measures was the same for both comparisons.

MTR data (pseudo-MS data) are statistically similar to the differences exhibited by the normal MTR data and the MS MTR data. Therefore, this normal-to-MS transform is illustrative of the physiological changes that exist between the set of normal brains and the set of MS brains. This transform suggests, in terms of global MTR values, that a decrease is found in the number of voxels with high MTR values, with the majority of this decrease occurring approximately at an MTR value of 0.5 (Fig 4). At this MTR value, for every four voxels representing an MTR of approximately 0.5 in the normal brains, only one voxel represents this MTR value in the MS brain. The number of voxels with other high MTR values (>0.3) also decrease, but to a lesser extent.

It was also observed that a higher number of voxels with MTR values less than 0.3 were found in the MS brain than in the normal brain; however, the increase in voxels with low MTR values does

not balance out the decrease in voxels with high MTR values. In general, in going from a normal to an MS brain, the gain in voxels with low MTR values was less than 15% of the loss in voxels with high MTR values.

Discussion

These results confirm some of the previous findings of van Buchem et al (13, 14); that is, that the MTR mean and peak significantly decrease in MS patients as compared with normal control patients. However, unlike the results presented in this study, their analysis did not find a decrease in the global MTR histogram mode. This difference is most likely the result of different pulse sequences and/or offset frequency of the saturation pulse used. It should be realized that the model described in Figure 4 is a function of the scanner hardware and software as well as the underlying physiological differences between the MS and the normal groups.

It is important to consider the effects of modeling a transform with the same data that will eventually be processed with that transform. In this study, a transform was created by matching the mean normal MTR histogram with the mean MS MTR histogram. Next, all normal MTR data were put through this transform to create pseudo-MS MTR data. A simple example can be illustrative as regards this technique: let the following list of numbers represent a mean parameter value from the set of normal data (1,2,2,1,1,2) and let the next list of numbers represent the mean value of this same parameter for the set of MS data (2,5,8,0,5,7). The means of the two sets are 1.5 and 4.5, respectively. By multiplying the first set by 3, one can arrive at a set of pseudo-MS data containing the same mean as the MS data; that is, (3,6,6,3,3,6). Using a Wilcoxon rank sum test, the normal and MS data are not significantly different ($P = .0592$), whereas the normal and the pseudo-MS sets are significantly different ($P = .0277$). Thus, even if one could assume that the matching of the mean histogram of the two groups would force the mean of all 30 of the examined parameters to be the same, it does not follow that the statistical analysis between the two groups can be predicted. Individual variations are an important factor, and it is for this reason that the normal and MS comparison is not identical to the normal and pseudo-MS comparison (Fig 6).

Finally, it would be interesting to investigate the effects of changing the histogram bin size. While the MTR values used to derive the simple statistics, the range statistics, and the order statistics are basically unlimited in resolution, this is not true of the histogram parameters, which are derived using binned MTR values. One potential problem is that the normal-to-MS transform was derived from the matching of the group mean histograms of the normal and MS subjects; therefore, an increase in histogram bin size will cause a decrease in transform resolution, which then decreases the resolution of the pseudo-MS data. Thus, the appearance of approximately smooth histograms for the normal, the MS, and the pseudo-MS data set (data not shown) indicated that the histogram bin size was appropriate, although, in general, a range of appropriate bin sizes can be found. As for the exact effect of different bin sizes on the found histogram parameters, this has not yet been investigated.

Conclusion

From the large number (17 of 30) of significantly different measures from the comparison of normal and MS data, MS does affect a large enough region as to be discernible through a global MTR analysis of a subject's complete brain. How this effect is occurring is still unknown, although an illustrative model of these differences can be created. In general, this normal-to-MS transform depicts a loss of voxels at high MTR values and a gain of voxels at low MTR values when going from a normal brain to an MS brain. This finding is in agreement with our previous study that showed a correlation between T2 lesion load and an increase in voxels with low MTR values (16). However, the transform also shows that the increase of voxels with low MTR values only makes up approximately 15% of the total decrease in voxels with higher MTR values, suggesting that the other 85% of this decrease is attributable to the loss of white matter over time, which could be related to MS brain atrophy (22). This is an interesting observation, because findings of recent serial studies of relapsing-remitting MS patients have shown that progressive brain atrophy occurs early in the disease and correlates with enhancing lesion activity (21, 22).

While this work has been based on each subject's mean value of each of the 30 measures, a longitudinal study of each of these measures over time would be a promising area for future work. This type of analysis may be more specific for evaluating treatment effects than other MR imaging measures, such as quantifying contrast-enhancing lesions and/or total white matter lesion load. For example, one may find treatments that affect some of the measures and not others. Use of the normal-to-MS transform may be informative in such a longitudinal study, since it provides a novel method of illustrating disease progression.

One other important area of future work would be the use of this type of transform to allow pooling of MTR data. Because of the dependence of magnetization transfer on scanner hardware and software, different scanners may provide very different MTR values for the same subject. In addition, after a software or hardware upgrade, previously acquired data must be analyzed separately from any newly acquired data, thus limiting statistical analysis. One potential solution to this problem is to use the mean MTR histograms of a set of normal subjects imaged on two different units (or

the same scanner after an upgrade) to create a normal-to-normal transform analogous to the creation of the normal-to-MS transform that was developed in this study. Since the two sets of normal data should not significantly differ, this normal-to-normal transform can be considered a scanner-to-scanner transform. In this way, all data acquired from one scanner can be transformed to appear as if they were acquired on another scanner, or all data acquired before an upgrade can be transformed to appear as if they were acquired after the upgrade.

Acknowledgments

We acknowledge Henry McFarland, Roger Stone, and the National Institute of Neurological Disease and Stroke for their participation in the ongoing NIH natural history study trial.

References

1. Dousset V, Grossman RI, Ramer KN, et al. **Experimental allergic encephalomyelitis and multiple sclerosis: lesion characterization with magnetization transfer imaging.** *Radiology* 1992;182: 483–491
2. Mehta RC, Pike GB, Enzmann D. **Measure of magnetization transfer in multiple sclerosis demyelinating plaques, white matter ischemic lesions, and edema.** *AJNR Am J Neuroradiol* 1996;17:1051–1055
3. Gass A, Barker GJ, Kidd D, et al. **Correlation of magnetization transfer ratio with clinical disability in multiple sclerosis.** *Ann Neurol* 1994;36:62–67
4. Tomiak MM, Rosenblum JD, Prager, Metz CE. **Magnetization transfer: a potential method to determine the age of multiple sclerosis lesions.** *AJNR Am J Neuroradiol* 1994;15:1569–1574
5. Lai HM, Davie CA, Gass A, et al. **Serial magnetization transfer ratios in gadolinium-enhancing lesions in multiple sclerosis.** *J Neurol* 1997;244:308–311
6. Hiehle JF, Grossman RI, Ramer KN, Gonzalez-Scarano F, Cohen JA. **Magnetization transfer effects in MR-detected multiple sclerosis lesions: comparison with gadolinium-enhanced spin-echo images and nonenhanced T1-weighted images.** *AJNR Am J Neuroradiol* 1995;16:69–77
7. Petrella JR, Grossman RI, McGowan JC, Campbell G, Cohen JA. **Multiple sclerosis lesions: relationship between MR enhancement pattern and magnetization transfer effect.** *AJNR Am J Neuroradiol* 1996;17:1041–1049
8. Loevner LA, Grossman RI, McGowan JC, Ramer KN, Cohen JA. **Characterization of multiple sclerosis plaques with T1-weighted MR and quantitative magnetization transfer.** *AJNR Am J Neuroradiol* 1995;1473–1479
9. Hiehle JF, Lenkinski RE, Grossman RI, et al. **Correlation of spectroscopy and magnetization transfer imaging in the evaluation of demyelinating lesions and normal appearing white matter in multiple sclerosis.** *Magn Reson Med* 1994;32:285–293
10. Kimura H, Grossman RI, Lenkinski RE, Gonzalez-Scarano R. **Proton MR spectroscopy and magnetization transfer ratio in multiple sclerosis: correlative findings of active versus irreversible plaque disease.** *AJNR Am J Neuroradiol* 1996;17:1539–1547
11. Filippi M, Campi MD, Dousset V, et al. **A magnetization transfer imaging study of normal-appearing white matter in multiple sclerosis.** *Neurology* 1995;45:478–482
12. Loevner LA, Grossman RI, Cohen JA, Lexa FJ, Kessler D, Kolso DL. **Microscopic disease in normal-appearing white matter on conventional MR images in patients with multiple sclerosis: assessment with magnetization-transfer measurements.** *Radiology* 1195;196:511–515
13. van Buchem MA, McGowen JC, Kolson DL, Polansky M, Grossman RI. **Quantitative volumetric magnetization transfer analysis in multiple sclerosis: estimation of macroscopic and microscopic disease burden.** *Magn Reson Med* 1996;36:632–636
14. van Buchem MA, Udupa JK, McGowan JC et al. **Global volumetric estimation of disease burden in multiple sclerosis based on magnetization transfer imaging.** *AJNR Am J Neuroradiol* 1997;18:1287–1290
15. van Buchem MA, Grossman RI, Armstrong C, et al. **Correlation of volumetric magnetization transfer imaging with clinical data in MS.** *Neurology* 1998;50:1609–1617
16. Richert ND, Ostuni JL, Bash CN, Duyn JH, McFarland HF, Frank JA. **Serial whole-brain magnetization transfer imaging in patients with relapsing-remitting multiple sclerosis at baseline and during treatment with interferon beta-1b.** *AJNR Am J Neuroradiol* 1998;19:1705–1713
17. Stone LA, Frank JA, Albert PS, et al. **The effect of interferon-beta on blood-brain barrier disruptions demonstrated by contrast-enhanced magnetic resonance imaging in relapsing/remitting multiple sclerosis.** *Ann Neurol* 1995;37:611–619
18. Ostuni JL, Levin RL, Frank JA, DeCarli C. **Correspondence of closest gradient voxels: A robust registration algorithm.** *J Magn Reson Imaging* 1997:7;410–415
19. Freund W. *Mathematical Statistics.* Englewood Cliffs, NJ: Prentice Hall; 1987
20. Pratt WK. *Digital Image Processing.* New York: Wiley; 1991: 559–561
21. Simon J, Jacobs LD, Campion M, Rudnick R. **A longitudinal study of brain atrophy in relapsing MS.** *Neurology* 1998; 50(Suppl 4):A192
22. Losseff NA, Wang L, Lai HM, et al. **Progressive cerebral atrophy in multiple sclerosis: a serial MRI study.** *Brain* 1996; 119:2009–2019